


RESEARCH PAPER



Regulation of *OCT2* transcriptional repression by histone acetylation in renal cell carcinoma

Qianying Zhu^{*a}, Lushan Yu^{*a}, Zhiyuan Qin ^a, Lu Chen^a, Haihong Hu^a, Xiaoli Zheng^b, and Su Zeng^a

^aInstitute of Drug Metabolism and Pharmaceutical Analysis, Zhejiang Province Key Laboratory of Anti-Cancer Drug Research, College of Pharmaceutical Sciences, Zhejiang University, Hangzhou, China; ^bHangzhou Cancer Institution, Hangzhou Cancer Hospital, Hangzhou, China

ABSTRACT

Renal cell carcinoma (RCC) is a common malignant tumour affecting the urinary system, and multidrug resistance is one of the major reasons why chemotherapy for this type of cancer often fails. Previous studies have shown that loss of the human organic cation transporter *OCT2* is the main factor contributing to oxaliplatin resistance in RCC, and that DNA hypermethylation and histone methylation play important roles in the transcriptional repression of *OCT2* in RCC. In this study, we found that histone acetylation also regulates *OCT2* repression in RCC and elucidated the underlying mechanisms. In normal renal cells, *HDAC7* combines with *MYC* at the *OCT2* promoter, resulting in a decrease in free *HDAC7*, which in turn increases the levels of H3K18ac and H3K27ac at the *OCT2* promoter and activates *OCT2* expression. In RCC cells, however, the interaction between *HDAC7* and *MYC* does not occur, which leads a high abundance of *HDAC7* and low levels of H3K18ac and H3K27ac at the *OCT2* promoter, thereby resulting in the inhibition of *OCT2* transcription. We found that combined treatment using the DNA methylation inhibitor decitabine and the histone deacetylase inhibitor vorinostat significantly increased the expression of *OCT2* in RCC cell lines, which sensitized these cells to oxaliplatin. We accordingly propose that the combination of anticancer agents and epigenetic drugs can provide a novel chemotherapeutic regimen.

ARTICLE HISTORY

Received 11 December 2018
Revised 16 April 2019
Accepted 26 April 2019

KEYWORDS

Renal cell carcinoma;
histone acetylation;
combination therapy;
epigenetic regulation; *OCT2*





Introduction

Worldwide, kidney cancer accounts for 2–3% of all cancers [1], and approximately 90% of the kidney cancers are renal cell carcinomas (RCCs) [2]. RCC is also one of the tumours prone to multidrug resistance (MDR). The effective rate of clinical chemotherapy for RCC is only 7–10%. This MDR can be attributed in part to the high expression of certain drug transporters in the kidney. The human organic cation transporter member 2 (*OCT2*, encoded by *SLC22A2*), which is the most abundant organic cation transporter in the kidney, is mainly expressed on the basolateral or apical side of renal tubular epithelial cells and participates in drug uptake [3–5]. The functions of this transporter are related to the disposal of many clinically endogenous substances and drugs in the body [6,7].


Previous studies have shown that platinum is the main anti-cancer substrate of *OCT2* [8], and

that *OCT2* has different transportability for different platinum compounds (in the order oxaliplatin > Pt [DACH]Cl₂ > ornaplatin > transplatin > cisplatin), whereas it is unable to transport carboplatin [9]. In addition, several studies have shown that an increase in the exogenous expression of *OCT2* can significantly increase the accumulation of oxaliplatin and thereby enhance cell cytotoxicity [10,11]. Although some other *OCT* transporters, such as *OCT1* [10] and *OCT3* [12], are also involved in the transport of platinum, the expression of these transporters in renal tubular epithelial cells is very low [10]. Therefore, the expression and activity of *OCT2* are assumed to play decisive roles in the accumulation and cytotoxicity of platinum anti-cancer drugs, particularly oxaliplatin, in renal cancer cells.

Histone acetylation, which is associated with chromatin assembly, DNA repair, and

CONTACT Xiaoli Zheng  gezixll@hotmail.com  Hangzhou Cancer Institution, Hangzhou Cancer Hospital, Hangzhou, China; Su Zeng  zengsu@zju.edu.cn
 Institute of Drug Metabolism and Pharmaceutical Analysis, Zhejiang Province Key Laboratory of Anti-Cancer Drug Research, College of Pharmaceutical Sciences, Zhejiang University, Hangzhou, China

*These authors contributed equally to this work.

 Supplemental data for this article can be accessed [here](#).

© 2019 Informa UK Limited, trading as Taylor & Francis Group

recombination [13,14], is one of the most extensively studied types of epigenetic modification. Dynamic histone acetylation is critical for correct gene expression and is regulated by a balance of histone acetyltransferases (HATs) and histone deacetylases (HDACs). If this balance is disrupted, there exists the potential for tumour development [15].

HATs include members of the p300/CBP and MYS GNAT families. It has been found that CBP and P300 catalyse the process whereby H3K18ac and H3K27ac activate the transcription of downstream genes [16]. On the basis of structural differences, HDACs can be divided into five classes: Class I, including HDAC1, HDAC2, HDAC3, and HDAC8; Class IIa, including HDAC4, HDAC5, HDAC7, and HDAC9; Class IIb, including HDAC6 and HDAC10; Class III, which are related enzymes of silent information regulator 2 (SirT2), and Class IV, which comprises only HDAC11. HDACs regulate tumour growth by inhibiting histone acetylation, which in turn suppresses the transcription of oncogenes [17]; therefore, HDACs can provide key targets for anti-tumour drugs. Vorinostat (suberoylanilide hydroxamic acid, SAHA) was the first HDAC inhibitor approved by the Federal Drug Administration (FDA) for the treatment of cutaneous T-cell lymphoma (CTCL), and thereafter Romidepsin (FK228) was also approved by the FDA for treatment of CTCL and peripheral T-cell lymphoma.

Previous studies have demonstrated that the loss of OCT2 in tumour cells is the major cause of oxaliplatin resistance in RCC. DNA and histone methylations are key factors in the transcriptional repression of *OCT2* in RCC [18]. Here, we found that aberrant histone acetylation also occurs in the *OCT2* promoter and explore the mechanisms whereby an *HDAC7-MYC* complex mediates the regulation of *OCT2* in RCC. Although epigenetic drugs have poor therapeutic effects on most solid tumours [19,20], the combination of epigenetic drugs with cytotoxic drugs [21] or immunotherapeutics [22] can enhance the anti-cancer effect, indicating that it is possible to design novel combination therapies for RCC. As *OCT2* expression is increased by the HDAC inhibitor SAHA and DNA methylation inhibitor decitabine (DAC) in RCC cells, we investigated the

synergistic effect of SAHA-DAC-oxaliplatin combination therapy on RCC cells.

Results

Aberrant active histone acetylation by H3K27ac and H3K18ac in RCC

OCT2 transcriptional repression in RCC has previously been shown to be regulated by DNA methylation and H3K4me3 [18]; however, to date, it was not known whether histone acetylation is related to *OCT2* transcriptional repression. We initially observed that in three pairs of the tumour-adjacent tissues, H3K18ac and H3K27ac were both enriched around the transcription start site (TSS) of the *OCT2* promoter, whereas H3K9ac abundance was very low (Figure 1(a)). As H3K18ac, H3K27ac, and H3K9ac are involved in transcriptionally permissive histone modification, the results indicated that H3K18ac and H3K27ac might be associated with *OCT2* transcription. We observed that *OCT2* transcription was markedly decreased in selected three pairs of RCC tissues (Figure 1(b)), and thus ChIP-qPCR assays were carried out to identify H3K18ac and H3K27ac occupancy in these three pairs of tissues. In the tumour-adjacent tissues, H3K18ac and H3K27ac were highly enriched around the TSS of *OCT2* and were reduced to different degrees in the matched tumour tissues, whereas no significant change was detected for H3K9ac (Figure 1(c–e)), indicating that the loss of H3K18ac and H3K27ac, but not that of H3K9ac, might occur at the *OCT2* promoter when *OCT2* is repressed in RCC.

Increased transcriptional expression of HDAC7 and HDAC9 in RCC

Given that the acetylation and deacetylation of histones are catalysed by HATs and HDACs, respectively, we next attempted to determine whether HATs or HDACs mediate *OCT2* repression in RCC.

The Oncomine database showed that the expression of *CBP* and *P300*, which have been reported to mainly catalyse H3K18ac and H3K27ac, had no significant effect in RCC tumours compared with the

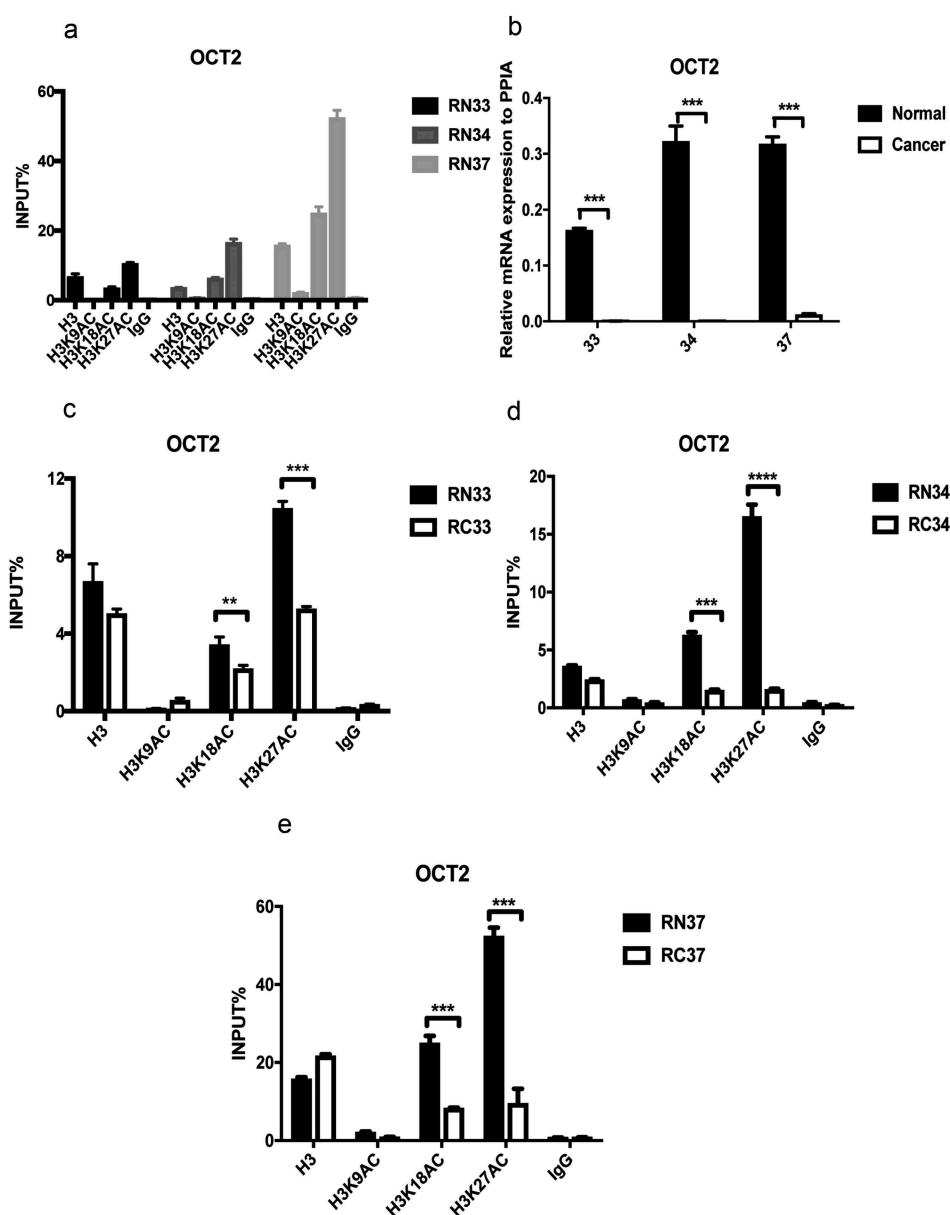


Figure 1. Decreased *OCT2* transcriptional expression and aberrant histone acetylation in three pairs of RCC patients tissues (No. 33;34;37). (a) ChIP assay of H3K9ac, H3K18ac and H3K27ac at *OCT2* promoter in tumour-adjacent kidney tissues; (b) RT-qPCR analysis of *OCT2* mRNA expression; (c, d, e) H3K9ac, H3K18ac and H3K27ac occupancy at *OCT2* promoter. The results are expressed as means \pm S.D. from technical triplicates in A-E [one-tailed unpaired t-test; ** $P < 0.01$; *** $P < 0.001$; **** $P < 0.0001$].

tumour-adjacent tissues (Fig. S1). The microarray data indicated that HDACs, but not *CBP* and *P300*, are the key factors involved in histone acetylation in RCC. To determine the role of HDACs in the *OCT2* regulatory mechanism, the mRNA expression of class I and II HDACs was examined in four randomly selected pairs of RCC tissues with reduced expression of *OCT2* (Figure 2(a), Fig. S2) by RT-qPCR. We found that only *HDAC7* and *HDAC9* were up-regulated in these four RCC tissues (Figure 2(b-e)), suggesting that these two HDACs

might mediate histone deacetylation around the TSS of the *OCT2* promoter. We then examined the mRNA expression of *HDAC7* and *HDAC9* in 36 pairs and 30 pairs of RCC tissues, respectively (Figure 2(f-g)); Fig. S3). Due to ethical reasons, the amounts of some of the collected samples were insufficient to enable mRNA expression analysis of both *HDAC7* and *HDAC9*. The results confirmed that higher *HDAC7* and *HDAC9* expression was detected in RCC tumours than in the paired adjacent tissues. Due to *OCT2* repression in RCC, the

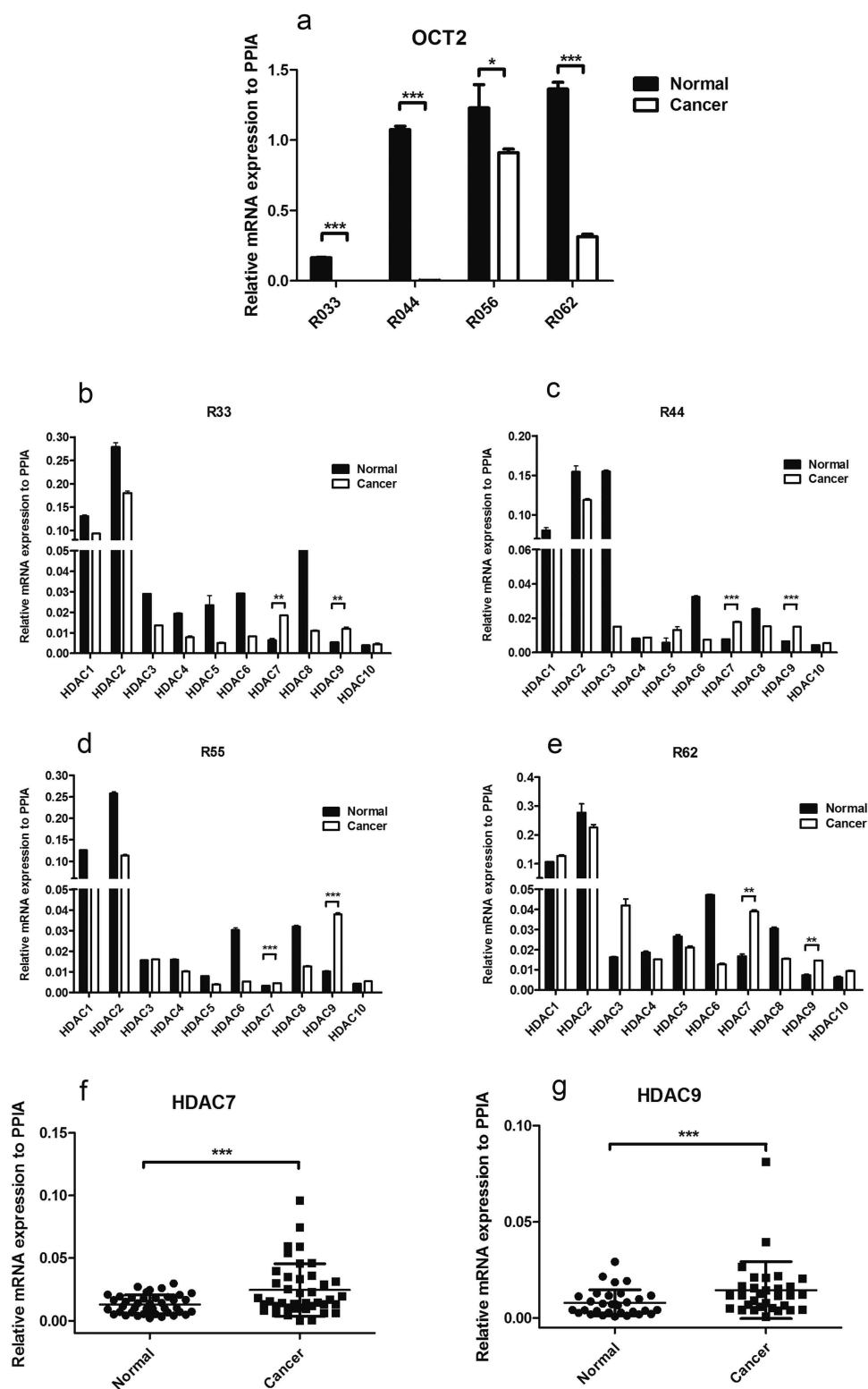


Figure 2. HDACs transcriptional expression in RCC patients tissues. (a) RT-qPCR analysis of *OCT2* mRNA expression in four pairs of RCC patient tissues (No. 33,44,55,62); (b, c, d, e) RT-qPCR analysis of HDACs mRNA expression in four pairs of RCC patient tissues (No. 38,44,55,62); (f, g) The two-tailed paired t-test for mRNA expression of *HDAC7* (f) and *HDAC9* (g) in RCC tissues. The results are expressed as means \pm S.D. from technical triplicates in a–f [a–e: one-tailed unpaired t-test: * $P < 0.1$; ** $P < 0.01$; *** $P < 0.001$; **** $P < 0.0001$; F-G: two-tailed paired t-test: **** $P < 0.001$].

assembled data further indicated that *HDAC7* and *HDAC9* regulate the abundance of H3K27ac and H3K18ac at the *OCT2* promoter, resulting in a decrease in H3K18ac and H3K27ac in RCC.

Increased HDAC7 occupancy upon SAHA treatment and myc-mediated activation of *OCT2*

In order to examine the influence of histone acetylation on *OCT2* expression, 786-O cells were treated with the histone deacetylase inhibitor SAHA. We accordingly observed that *OCT2* expression was activated in 786-O cells in response to SAHA treatment (Figure 3(a)). As SAHA inhibits all class I and II HDACs, to further investigate how *HDAC7* and *HDAC9* affected *OCT2* expression, 786-O cells were transfected with nontargeting control siRNA (si-NC), or siRNA targeting *HDAC7* (siHDAC7-s1 and siHDAC7-s2) and *HDAC9* (siHDAC9-s1 and siHDAC9-s2). The silencing effect of siRNA was assessed by RT-qPCR (Figure 3(c–d)). After transient knockdown expression of *HDAC7* and *HDAC9*, *OCT2* expression was significantly increased in 786-O cells (Figure 3(b)), and *OCT2* protein expression was increased after *HDAC7* and *HDAC9* knockdown in 786-O cells (Figure 3(e–f)). Collectively, these results provide evidence that both *HDAC7* and *HDAC9* regulate *OCT2* expression in RCC. In addition, the expression of *OCT2* was found to be positively correlated with the efficiency of HDAC inhibition.

Our previous data have indicated that *MYC*, acting as a transcription factor, regulates *OCT2* expression by binding to the *OCT2* promoter [18]. In our study, we found SAHA induces the mRNA expression of *MYC* in 786-O (Figure 4(a)). We therefore generated 786-O cells that stably expressed shRNA against *MYC* as described in a previous study [18]. *MYC* was efficiently knocked down when shRNA against *MYC* was turned on by doxycycline treatment (Figure 4(b)). The knockdown of *MYC* was found to block the transcriptional activation of *OCT2* by SAHA in both mRNA and protein level (Figure 4(c–d)). We then performed Co-IP analysis to examine the direct interaction between *MYC* and *HDAC7* in 786-O cells following treatment with SAHA. We found that *MYC* and *HDAC7* bind to

each other after SAHA treatment, and when *MYC* was knocked out, the protein complex disappeared, but there was still free *HDAC7* in the cell (Figure 4(e)). However, *HDAC9* did not bind to *MYC* in SAHA-treated 786-O cells (Fig. S4). A subsequent CHIP-qPCR assay showed that both *MYC* and *HDAC7* occupancy at the E-box of the *OCT2* promoter were enriched in SAHA-treated 786-O cells (Fig. S5), resulting in the reducing of free *HDAC7* at the acetylation site of *OCT2* promoter (Figure 4(f)). When *HDAC7* was knocked down, H3K18ac and H3K27ac enriched at *OCT2* promoter in 786-O cells (Figure 4(g)). We accordingly proposed our assumption that the combination of *MYC* and *HDAC7* at the E-box of *OCT2* promoter in normal renal cells results in a decrease in free *HDAC7*, which may increase the expression H3K18ac and H3K27ac and activate *OCT2* transcription. In contrast to normal kidney cells, *MYC* cannot bind to and interfere with *HDAC7* in RCC cells, which increases the amounts of free *HDAC7* at the *OCT2* promoter and decreases H3K18ac and H3K27ac levels, eventually resulting in *OCT2* transcriptional inhibition. However, it remains unclear why the recruitment of *HDAC7* by *MYC* at the *OCT2* promoter in RCC cells is disrupted.

Combination therapy using epigenetic drugs and oxaliplatin enhances the chemosensitivity of RCC cells

Previous studies have shown that DAC can effectively induce the expression of *OCT2* and that sequential combination of DAC and oxaliplatin sensitizes RCC cells to oxaliplatin both in vitro and in xenografts [18]. In our study, we observed a 28.4-fold increase in epigenetic activation of *OCT2* in RCC cells following DAC+SAHA treatment (Figure 5(a)). The rank order of induction was as follows: DMSO > SAHA > DAC > DAC+SAHA in both mRNA and protein level (Figure 5(a–b)). The platinum cellular uptake in 786-O has the same trend as *OCT2* up-regulated expression (Figure 5(c)). We therefore examined whether pretreatment with DAC and SAHA synergistically promoted stronger cytotoxicity compared with DAC or SAHA alone. Cells of the 786-O line were initially treated sequentially with increasing

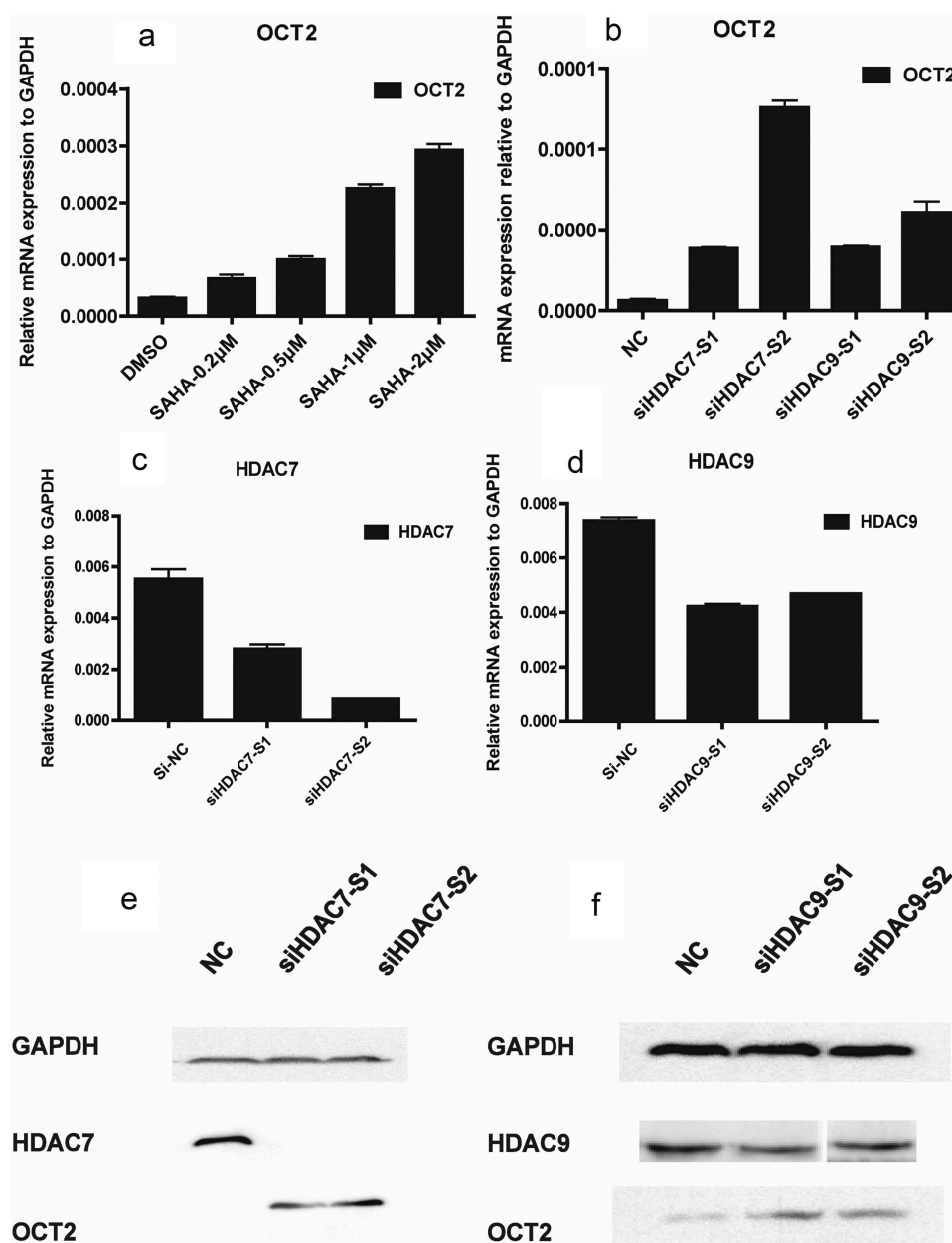


Figure 3. Loss of *HDAC7/HDAC9* up-regulated the expression of *OCT2* in RCC cell line 786-O. (a) RT-qPCR analysis of *OCT2* mRNA expression in 786-O after treated with SAHA at 0.2 μ M, 0.5 μ M, 1.0 μ M, 2.0 μ M for 48 h; (b) RT-qPCR analysis of *OCT2* mRNA expression after *HDAC7* or *HDAC9* knocked down in 786-O cells; (c, d) RT-qPCR analysis of *HDAC7* (c) or *HDAC9* (d) mRNA expression after targeted siRNA was transfected into 786-O cells. (e) *HDAC7* and *OCT2* protein expression after *HDAC7* knockdown in 786-O cells. (f) *HDAC9* and *OCT2* protein expression after *HDAC9* knockdown in 786-O cells. The results are expressed as means \pm S.D. from technical triplicates in A-D.

concentrations of SAHA, DAC, or oxaliplatin (Fig. S6A). The median inhibitory concentration (IC_{50}) values of these three drugs were calculated as follows: IC_{50} (DAC) = 12.01 μ M, IC_{50} (SAHA) = 4.69 μ M, and IC_{50} (oxaliplatin) = 22.39 μ M (Fig. S6B-D). Finally, the 786-O cells were pretreated sequentially with increasing concentrations of SAHA and/or DAC, followed by application of various concentrations of oxaliplatin at 48

h (Supplemental Table 4) to evaluate the combination index (CI). According to the Chou-Talalay method, the gradient concentrations of drugs are determined by their IC_{50} values [23]. As shown in Figure 5(d), DAC and oxaliplatin alone induced an approximate 50% reduction in the survival rate of 786-O cells at maximal concentrations of 50 μ M and 150 μ M, respectively, whereas SAHA had a 70–80% cytotoxic effect at the maximal

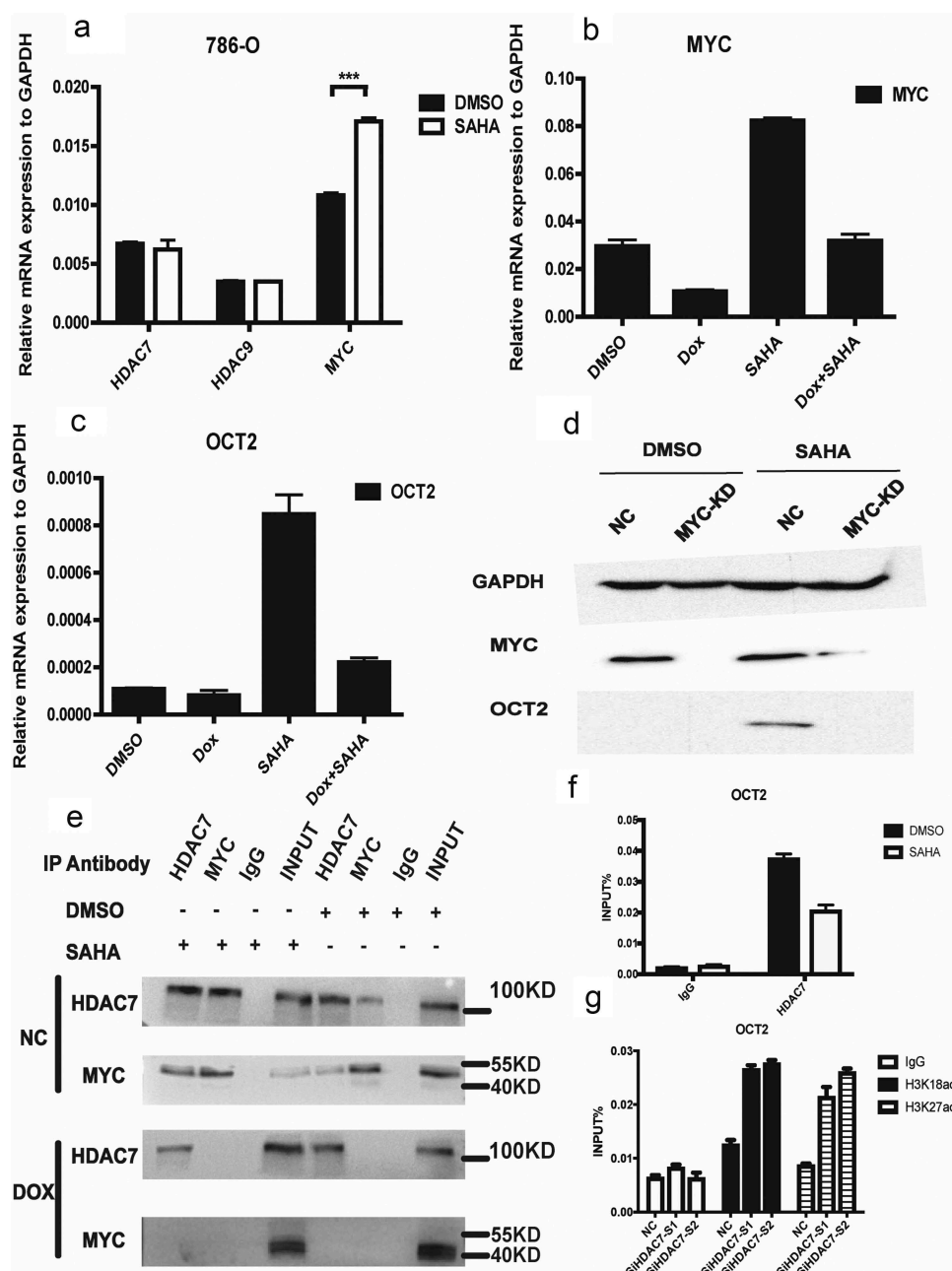


Figure 4. MYC combined with HDAC7 at OCT2 promoter to regulate the OCT2 expression in RCC cell line 786-O. (a) RT-qPCR analysis of HDAC7, HDAC9 and MYC mRNA expression in 786-O after treated with 2 μ M SAHA for 48 h; (b, c) RT-qPCR analysis of MYC (b) and OCT2 (c) mRNA expression in 786-O cells after knockdown MYC and treated with 2 μ M SAHA for 48 h; (d) MYC and OCT2 protein expression in 786-O cells after knockdown MYC and treated with 2 μ M SAHA for 48 h. (e) Co-IP analysis of HDAC7-MYC complex in 786-O cells after knockdown MYC and treated with 2 μ M SAHA for 48 h; (f) ChIP-qPCR analysis of HDAC7 enrichment at OCT2 promoter in 786-O cells after treated with 2 μ M SAHA for 48 h; (g) ChIP-qPCR analysis of H3K18ac and H3K27ac enrichment at OCT2 promoter in 786-O cells after HDAC7 knockdown. The results are expressed as means \pm S.D. from technical triplicates in a, b, c, f, g [a: one-tailed unpaired t-test: P = 0.0008].

concentration of 20 μ M. Given that it is essentially unproductive to examine the effects of drug combinations when the cell growth inhibition is extremely low, we only investigated the effect of such combinations when the cell growth inhibition rate was greater than 50%. Whereas a synergistic or additive effect was observed after treatment of

786-O cells with SAHA+oxaliplatin (CI = 0.29–0.89), only synergistic effects were observed after 786-O cells had been treated with DAC+oxaliplatin and DAC+SAHA+oxaliplatin (CI_{DAC+OXA} = 0.12–0.47, CI_{DAC+SAHA+OXA} = 0.11–0.63). In order to compare the synergistic effect of DAC+oxaliplatin and DAC+SAHA

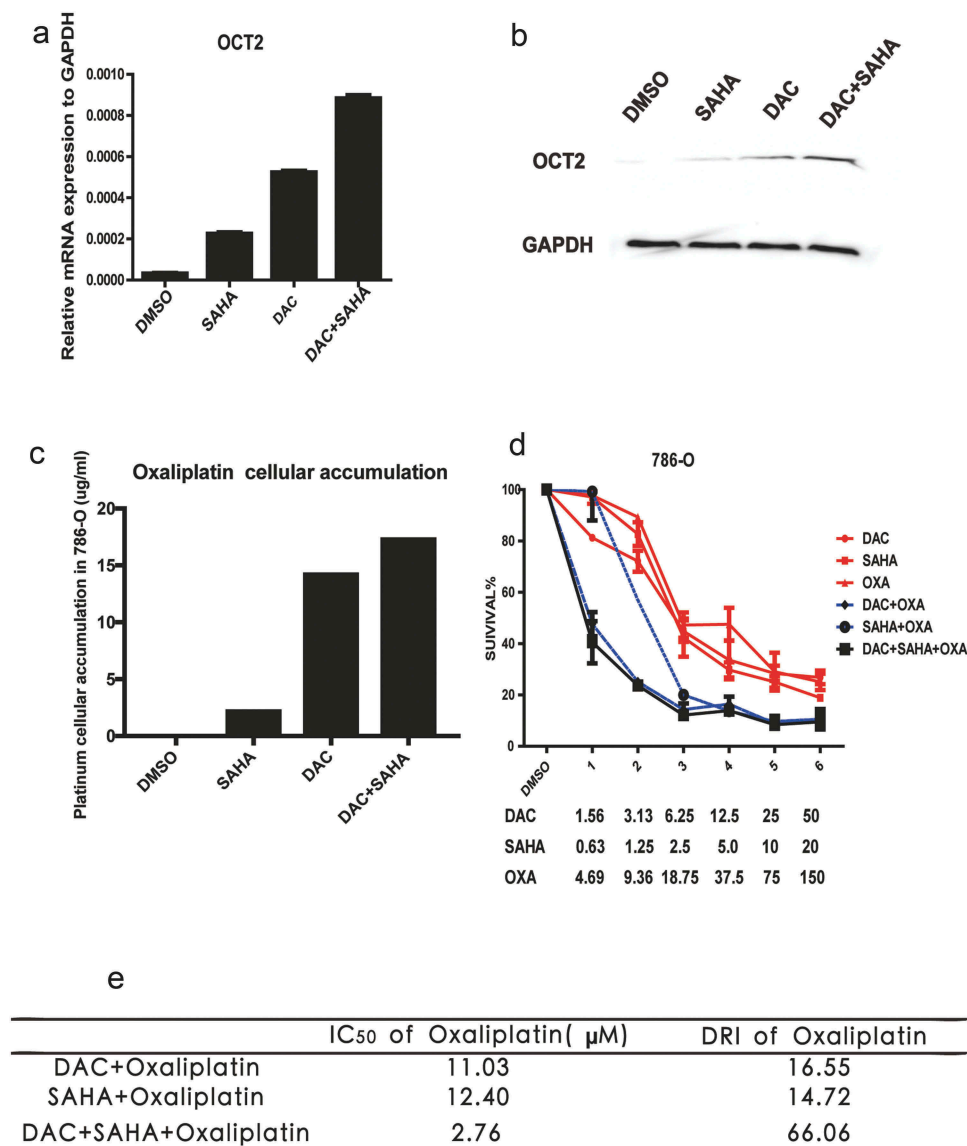


Figure 5. DAC, SAHA and oxaliplatin combinations. (a) RT-qPCR analysis of *OCT2* mRNA expression after treated with DAC, SAHA and DAC+SAHA in 786-O cells, respectively; (b) *OCT2* protein expression of DAC, SAHA, DAC+SAHA treatment in 786-O cells; (c) Platinum cellular accumulation after treated with DAC, SAHA and DAC+SAHA in 786-O; (d) Dose-Survival Curve of DAC, SAHA, OXA, DAC+SAHA, DAC+OXA, SAHA+OXA, DAC-SAHA-OXA in 786-O cells; (e) The IC₅₀ and dose-reduction index (DRI) of OXA. DRI is the ratio of dose of OXA (alone) to dose of OXA (combo), which represents the fold-dose decrease of OXA in combination. CI < 0.8, 0.8 < CI < 1, and CI > 1 indicate synergism, additive effect, and antagonism, respectively. The results are expressed as means \pm S.D. from technical triplicates in a–d.

+oxaliplatin in 786-O cells, we calculated the IC₅₀ value and dose-reduction index (DRI) of oxaliplatin in 786-O cells (Figure 5(e)), where DRI is the ratio of the dose of oxaliplatin_(alone) to the dose of oxaliplatin_(combo), which represents the fold-dose decrease in oxaliplatin in combination. As shown in Figure 5(e), the DRI_(oxaliplatin) of DAC+SAHA+oxaliplatin was clearly higher than that of the other combinations, indicating that pretreatment of 786-O cells with DAC+SAHA followed by treatment with oxaliplatin had the strongest synergistic

cytotoxicity compared with any other combination.

Discussion

Many renal masses remain asymptomatic or non-palpable until the advanced stages of RCC [1]. The 5-year survival rate for patients with metastatic RCC is less than 10% [24], with the low survival rate being attributable to the high resistance of RCC to both chemotherapy and radiation therapy [25]. Such

resistance to chemotherapy can often be ascribed to MDR mediated by drug transporters [26,27].

OCT2 is an uptake transporter expressed in kidney tubules. In our previous studies, we detected a correlation between the loss of OCT2 expression and tumour cell resistance to platinum, which showed that the aberrant *OCT2* promoter in RCC is characterized by a hypermethylated CpG island and low H3K4 tri-methylation occupancy. In the present study, we further investigated other epigenetic factors related to OCT2 repression. We accordingly detected significant decreases in H3K18ac and H3K27ac at the *OCT2* promoter in RCC tumour tissue compared with the matched adjacent tissue (Figure 1(c–e)). H3K18ac and H3K27ac are involved in a variety of physiological processes and the relative balance between histone acetylation and deacetylation is essential for normal cell growth. The findings of a previous study have indicated that loss of H3K18ac causes suppression of the nonreceptor tyrosine kinase EtK, which plays an essential role in prostate cancer cell survival and growth [28], whereas disruption of the association between BRD4 and H3K27ac has been shown to downregulate MYC and promote antitumour activity in pre-clinical animal models of human cancers [29]. We therefore hypothesize that OCT2 repression in RCC may be attributable to the loss of H3K18ac and H3K27ac. However, on the basis of our present results, we cannot exclude the possibility that other HATs are involved in the transcriptional regulation of OCT2, and this accordingly warrants further research.

Histone acetylation is co-regulated by HATs and HDACs. HATs promote acetylation to generate less condensed chromatin structures, thereby enabling the activation of transcription, whereas HDACs mediate chromatin aggregation [30]. In the present study, we found that, compared with paired adjacent tissues, the expression of *HDAC7* and *HDAC9* increased in most of the RCC tissues, whereas the expression of other HDACs varied. These abnormal increases occurred during the early stage of RCC pathological grading, suggesting that *HDAC7* and *HDAC9* may be potential targets and early diagnostic markers for the treatment of RCC. Furthermore, we also speculated that the loss of H3K18ac and H3K27ac at the *OCT2* promoter is caused by *HDAC7/9*. It has been reported that the expression

of class I HDACs in tumours is abnormally increased at both the mRNA and protein levels when compared with paired adjacent tissues. In contrast to class I HDACs, expression of class II HDACs has been found to decrease in tumours, and a higher expression of class II HDACs predicts a better prognosis in patients [31]. *HDAC7* and *HDAC9* belong to class II HDACs and Osada et al. [32] found that *HDAC7* mRNA expression was higher in node-negative, low-grade lymph tumours compared with late-stage lymph node metastases. Furthermore, in pancreatic cancer, both the mRNA and protein expression levels of *HDAC7* are significantly up-regulated in tumours [33]. These studies therefore indicate that the expression of HDACs differs among different cancer types.

Histone deacetylation, and particularly the inhibitors of HDACs, has been a hot topic in anti-cancer drug research in recent years [34]. The SAHA we used in this study is a hydroxamic acid and has the characteristics of a longer half-life, lower toxicity, and greater stability compared with other hydroxamic acids such as TSA [31]. In 2006, the FDA gave approval for the use of SAHA in the treatment of cutaneous T-cell lymphomas. However, although it can induce the expression of *OCT2* mRNA in 786-O cells (Figure 3(a)), it does not induce such expression in other RCC cell lines, 769-P or CAKI (Fig. S7), which indicated the limitation of our study: the SAHA induction mechanism we studied may only work in certain part of RCC patients. Although the three cell lines are derived from primary renal clear cell carcinomas, they were obtained from different patients, which suggests different factors such as the oxygen content in the tumour microenvironment affecting the regulatory mechanism.

In our study, SAHA slightly up-regulated *MYC* in 786-O cells, whereas *MYC* itself can recruit both HATs and HDACs. Recent studies have shown that the recruitment of HATs by *MYC* may be mediated by TRRAP [35], which is not a HAT but is present in a different macro-molecular complex containing HAT sub-units, including GCN5, PCAF, and TIP60 [36]. *MYC* also recruits HDACs to gene promoters, and it has previously been demonstrated that *MYC* recruits *HDAC3* to form a transcriptional suppressor complex, co-localizes on the miR-451 promoter, and finally induces its downregulation in acute myeloid leukaemia [37]. However, on the basis of

the findings of the present study, we speculate that *MYC* performed an opposite function in complex recruitment in normal renal cells. As epigenetic regulation invariably involves the functioning of several different pathways, there are likely to be complex interactions relating to DNA methylation and HDACs. Previous studies have shown that synergy between HDAC activity and DNA methylation is operative for a key epigenetic abnormality in cancer cells, namely, transcriptional silencing of tumour suppressor genes [38].

Based on the above results, we propose a hypothesis that the histone acetylation mechanism underlying *OCT2* repression in RCC is regulated by the enrichment of free *HDAC7* at *OCT2* promoter (Figure 6). In normal renal cells, *HDAC7* combines with *MYC* at the E-box site on *OCT2* promoter, resulting in a decrease of free *HDAC7*s at the promoter, which increases H3K18ac and H3K27ac at the promoter and activates *OCT2* expression. However, in RCC cells, the *HDAC7*-*MYC* complex is not established, leading to an increase in free *HDAC7*s at the *OCT2* promoter and a decrease in the levels of H3K18ac and H3K27ac, thereby resulting in *OCT2* transcriptional inhibition.

It has previously been shown that the cellular accumulation of oxaliplatin is the key determinant of the cytotoxicity of this drug [39]. In renal cells, oxaliplatin is mainly bound by *OCT2* and effluxed

by *MATE-2K* [40]. Both *OCT2* and *MATE-2K* are repressed in RCC, whereas treatment with DAC or SAHA can induce the expression of *OCT2* but not *MATE-2K*, resulting in the high accumulation and cytotoxicity of OXA in RCC cells [18]. TSA, which is similar to SAHA, can up-regulate both *OCT2* and *MATE-2K* [41], and is hence not suitable for use in combination therapy.

HDACs have a potent effect in haematological diseases or lymphoid malignancies alone, but often fail to achieve satisfactory therapeutic effects in the case of solid tumours. In our study, we also found that synergistic effects of the SAHA-oxaliplatin combination were the lowest among the three combination groups examined, indicating that SAHA does not work well in combination with oxaliplatin. This may be related to the fact that SAHA does not cause a sufficiently high induction of *OCT2*. Therefore, a combination of DAC and SAHA has been used for tumour treatment. Chen et al. [42], for example, found that the combination of DAC and SAHA inhibited ovarian cancer growth by inducing apoptosis, G2/M arrest, autophagy, and re-expression of imprinted tumour suppressor genes, whereas Dong et al. [43] demonstrated that combined treatment with DAC and SAHA enhanced the antiproliferative activity of glioma cells. In our study, we designed a clinical protocol based on the combined use of DAC, SAHA, and the anti-cancer drug oxaliplatin, and we demonstrated that the toxicity of DAC+SAHA+oxaliplatin to 786-O cells was higher than that of DAC+oxaliplatin, and that the synergistic effect of this combination was stronger than that of DAC+oxaliplatin at high dose. Nowadays, there is a heightened focus on multidrug combination research in an effort to solve the pervasive problem of MDR. In this study, we found that DAC and SAHA significantly induced the expression of *OCT2* in RCC cells, enhanced the cellular accumulation of oxaliplatin, and significantly reversed drug resistance, thereby providing new insights for the revision of clinical oxaliplatin guidelines for RCC.

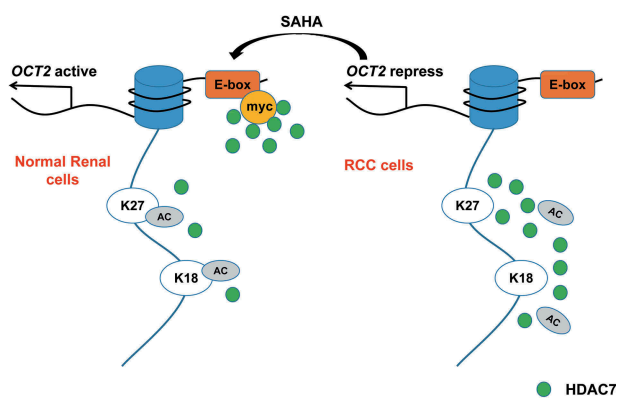


Figure 6. Histone acetylation mechanism of *OCT2* repression in RCC. In normal renal cells, *HDAC7* combines with *MYC* at the E-box site on *OCT2* promoter, resulting in a decrease of free *HDAC7*s at the promoter, which increases H3K18ac and H3K27ac at the promoter and activates *OCT2* expression. However, in RCC cells, the *HDAC7*-*MYC* complex is not established, leading to an increase in free *HDAC7*s at the *OCT2* promoter and a decrease in the levels of H3K18ac and H3K27ac, thereby resulting in *OCT2* transcriptional inhibition.

Materials and methods

Tissues and cell culture

Thirty-six paired tissue samples of RCC patients were provided by the Specimen Bank of Zhejiang Cancer Hospital (Hangzhou, China) and were approved by

the Institutional Review Board of Zhejiang Cancer Hospital [No. (2014)-08-76; for detailed patient information, see Supplemental Table 1].

HEK293T cells and cells of the RCC cell line 786-O were purchased from the Chinese Academy of Science Committee on Type Culture Collection Cell Libraries. HEK293T cells were cultured in Dulbecco's modified Eagle's medium containing 10% fetal bovine serum, and those of the 786-O line were cultured in RPMI-1640 medium containing 10% fetal bovine serum. All cells were maintained at 37°C in 5% CO₂. For epigenetic drug treatment, the 786-O cells were cultured in medium containing SAHA (Selleck Chemical) for 48 h or DAC (Sigma-Aldrich) for 72 h, with the medium being refreshed every 24 h.

Real-time quantitative polymerase chain reaction analysis

Total RNA of tissues was isolated using a total RNA mini-prep kit (Tiangen, Beijing, China), whereas total RNA from cell lines was isolated using a total RNA mini-prep kit (Axygen, Suzhou, China). The isolated RNA was subsequently reverse transcribed to cDNA using PrimeScript RT Master Mix (Takara, Tokyo, Japan). We performed real-time quantitative polymerase chain reactions (RT-qPCR) using a StepOnePlus System (Applied Biosystems) and SYBR Premix EX Taq (Takara, Tokyo, Japan). Peptidylprolyl isomerase A (*PPIA*) in tissues and glyceraldehyde-3-phosphate dehydrogenase (*GAPDH*) in cell lines served as the respective internal controls. The relative mRNA expression levels were normalized to *PPIA* or *GAPDH*. The sequences of the primers used for amplification are listed in Supplemental Table 2.

Short hairpin RNA transfection of the RCC cell line 786-O

Short hairpin RNAs (shRNAs) were cloned as described by Paddison et al. [44], and inserted into pTRIPZ lentiviral vectors (Thermo Scientific, Waltham, MA). To package virus, HEK293T cells were transfected with shRNA against MYC (shRNA-MYC) using Lipofectamine 2000 (Life Technologies, Grand Island, NY) according to the manufacturer's instructions. Cells of the 786-O line were infected by the supernatant virus of HEK293T cells. The sequences of the shRNAs used are listed in Supplemental Table 3. Cells of the 786-O line

expressed shRNA following treatment with 1 µg/mL doxycycline for 48 h.

Small interfering RNA transfection

The small interfering RNAs (siRNAs) were synthesized by GenePharma (Shanghai, China) and transfected into cells for 48 h using Lipofectamine 3000 (Life Technologies, Waltham, MA) according to the manufacturer's instructions. The target sequences of the siRNAs used are listed in Supplemental Table 3.

Chromatin immunoprecipitation assay (ChIP)

The procedures used for ChIP analysis have been described previously [45]. RT-qPCR was performed using the specific primers listed in Supplemental Table 2. The antibodies used for ChIP were as follows: anti-H3 (Abcam, Cambridge, MA; Ab1791), anti-H3K9ac (Abcam, Cambridge, MA; Ab4441), anti-H3K18ac (Abcam, Cambridge, MA; Ab1191), anti-H3K27ac (Abcam, Cambridge, MA; ab4729), anti-HDAC7 (Sigma, H2662), anti-MYC (Abcam, Cambridge, MA; ab32072), anti-HDAC9 (Abcam, Cambridge, MA; ab59718), and normal rabbit IgG (Santa Cruz Biotechnology, Santa Cruz, CA; sc-2027) as a control. The IP beads used were Anti-Rabbit Ig IP Agarose Beads (Rockland, 00-8800-25).

Co-immunoprecipitation (Co-IP)

For co-immunoprecipitation, we used previously described procedures [46] with some modifications. Briefly, a lysis buffer (20 mM Tris-HCl, pH 8.0, 300 mM NaCl, 0.5 mM EDTA, 1% Nonidet P-40, 1% Triton X-100) containing protease inhibitors was prepared freshly to lyse cells for immunoprecipitation. The lysate, together with the aforementioned antibodies and IP beads were incubated overnight at 4°C. The beads were then washed three times with IP lysis buffer and boiled in 2 × SDS loading buffer to elute the bound complexes. Western blotting was performed to determine the Co-IP results.

MTT assay

Cells of the 786-O line were seeded in 96-well plates at a density of 1000 cells/well, cultured for 24 h before drug treatment (see in Supplemental Table 4), and maintained in drug-free medium for 48 h. Thereafter, 100 µL of fresh medium containing 0.5 mg/mL MTT

was added to each well of the 96-well plate as described previously [47]. The DAC, SAHA, and oxaliplatin contents in 786-O cells were maintained at a constant molar ratio of 2.5:1:7.5 based on the potency (IC_{50}) of each drug. Drug synergy quantification was analysed using Compusyn software (ComboSyn, Inc.) according to the Chou-Talalay method [23]. The combined drug effects were quantified using the combination index (CI), where $CI < 0.8$, $0.8 < CI < 1.2$, and $CI > 1.2$ indicated synergism, additive effect, and antagonism, respectively.

Platinum cellular uptake in 786-O

Cells of the 786-O line were seeded in 6 cm cee dishes. After OCT2 expression was induced by DAC, SAHA or DAC+SAHA, 100 μ M oxaliplatin was administered for 24 h. The platinum cellular uptake was detected by ICP-MS, completed by Hangzhou Leading Pharmatech Co., Ltd.

Statistical analysis

A two-tailed paired t-test was used to analyse differences in *HDAC7/HDAC9* expression between RCC tissues and tumour-adjacent tissues. Multiple t-tests were used to evaluate differences in the expressions of *MYC*, *HDAC7*, and *HDAC9* determined by RT-qPCR and histone acetylation enrichment in ChIP assays. A P value of less than 0.05 was considered significant. All statistical analyses and drug IC_{50} calculations were performed using Prism version 6.0.

Disclosure statement

No potential conflict of interest was reported by the authors.

Funding

This project was supported by National Natural Science Foundation of China [81773817], National Key R&D Program of China [No. 2017YFC0908600, 2017YFE0102200], and the National Natural Science Foundation of China [No. 81702801].

ORCID

Zhiyuan Qin  <http://orcid.org/0000-0003-0824-5638>

References

- [1] Ljungberg B, Cowan NC, Hanbury DC, et al. EAU guidelines on renal cell carcinoma: the 2010 update. *Eur Urol*. 2010;58(3):398–406.
- [2] Baldewijns MM, van Vlodrop IJ, Schouten LJ, et al. Genetics and epigenetics of renal cell cancer. *Biochim Biophys Acta*. 2008;1785(2):133–155.
- [3] Gorboulev V, Ulzheimer JC, Akhoundova A, et al. Cloning and characterization of two human polyspecific organic cation transporters. *DNA Cell Biol*. 1997;16(7):871–881.
- [4] Motohashi H, Sakurai Y, Saito H, et al. Gene expression levels and immunolocalization of organic ion transporters in the human kidney. *J Am Soc Nephrol*. 2002;13(4):866–874.
- [5] Prasad B, Johnson K, Billington S, et al. Abundance of drug transporters in the human kidney cortex as quantified by quantitative targeted proteomics. *Drug Metab Dispos*. 2016;44(12):1920–1924.
- [6] Koepsell H, Gorboulev V, Arndt P. Molecular pharmacology of organic cation transporters in kidney. *J Membr Biol*. 1999;167(2):103–117.
- [7] Pritchard JB, Miller DS. Renal secretion of organic anions and cations. *Kidney Int*. 1996;49(6):1649–1654.
- [8] Budiman T, Bamberg E, Koepsell H, et al. Mechanism of electrogenic cation transport by the cloned organic cation transporter 2 from rat. *J Biol Chem*. 2000;275(38):29413–29420.
- [9] Burger H, Zoumaro-Djayoon A, Boersma AW, et al. Differential transport of platinum compounds by the human organic cation transporter hOCT2 (hSLC22A2). *Br J Pharmacol*. 2010;159(4):898–908.
- [10] Zhang S, Lovejoy KS, Shima JE, et al. Organic cation transporters are determinants of oxaliplatin cytotoxicity. *Cancer Res*. 2006;66(17):8847–8857.
- [11] Yao Z, Guo H, Yuan Y, et al. Retrospective analysis of docetaxel, oxaliplatin plus fluorouracil compared with epirubicin, cisplatin and fluorouracil as first-line therapy for advanced gastric cancer. *J Chemother*. 2014;26(2):117–121.
- [12] Yokoo S, Masuda S, Yonezawa A, et al. Significance of organic cation transporter 3 (SLC22A3) expression for the cytotoxic effect of oxaliplatin in colorectal cancer. *Drug Metab Dispos*. 2008;36(11):2299–2306.
- [13] McMurry MT, Krangel MS. Pillars article: a role for histone acetylation in the developmental regulation of V(D)J recombination. *Science*. 2000;287:495–498.
- [14] Wurtele H, Li Q, Zhou H, et al. Histone acetylation and chromatin assembly. *Med Sci*. 2009;25(2):121–122.
- [15] Dedes KJ, Dedes I, Imesch P, et al. Acquired vorinostat resistance shows partial cross-resistance to ‘second-generation’ HDAC inhibitors and correlates with loss of histone acetylation and apoptosis but not with altered HDAC and HAT activities. *Anticancer Drugs*. 2009;20(5):321–333.

- [16] Jin Q, Yu LR, Wang L, et al. Distinct roles of GCN5/PCAF-mediated H3K9ac and CBP/p300-mediated H3K18/27ac in nuclear receptor transactivation. *Embo J*. 2011;30(2):249–262.
- [17] Li Y, Seto E. HDACs and HDAC inhibitors in cancer development and therapy. *Cold Spring Harb Perspect Med*. 2016;6(10):a026831.
- [18] Liu Y, Zheng X, Yu Q, et al. Epigenetic activation of the drug transporter OCT2 sensitizes renal cell carcinoma to oxaliplatin. *Sci Transl Med*. 2016;8(348):348r–97r.
- [19] Stewart DJ, Issa JP, Kurzrock R, et al. Decitabine effect on tumor global DNA methylation and other parameters in a phase I trial in refractory solid tumors and lymphomas. *Clin Cancer Res*. 2009;15(11):3881–3888.
- [20] Ljungberg B, Bensalah K, Canfield S, et al. EAU guidelines on renal cell carcinoma: 2014 update. *Eur Urol*. 2015;67(5):913–924.
- [21] Fang F, Balch C, Schilder J, et al. A phase 1 and pharmacodynamic study of decitabine in combination with carboplatin in patients with recurrent, platinum-resistant, epithelial ovarian cancer. *Cancer*. 2010;116(17):4043–4053.
- [22] Chiappinelli KB, Zahnow CA, Ahuja N, et al. Combining epigenetic and immunotherapy to combat cancer. *Cancer Res*. 2016;76(7):1683–1689.
- [23] Chou TC. Drug combination studies and their synergy quantification using the Chou-Talalay method. *Cancer Res*. 2010;70(2):440–446.
- [24] Motzer RJ, Bander NH, Nanus DM. Renal-cell carcinoma. *New Engl J Med*. 1996;335(12):865.
- [25] Cohen HT, McGovern FJ. Renal-cell carcinoma. *New Engl J Med*. 2005;353(23):2477.
- [26] Fletcher JI, Haber M, Henderson MJ, et al. ABC transporters in cancer: more than just drug efflux pumps. *Nat Rev Cancer*. 2010;10(2):147–156.
- [27] Wang D, Lippard SJ. Cellular processing of platinum anticancer drugs. *Nat Rev Drug Discov*. 2005;4(4):307–320.
- [28] Dai B, Kim O, Xie Y, et al. Tyrosine kinase Etk/BMX is up-regulated in human prostate cancer and its over-expression induces prostate intraepithelial neoplasia in mouse. *Cancer Res*. 2006;66(16):8058–8064.
- [29] Sengupta D, Kannan A, Kern M, et al. Disruption of BRD4 at H3K27Ac-enriched enhancer region correlates with decreased c-Myc expression in Merkel cell carcinoma. *Epigenetics*. 2015;10(6):460–466.
- [30] Lehrmann H, Pritchard LL, Harel-Bellan A. Histone acetyltransferases and deacetylases in the control of cell proliferation and differentiation. *Adv Cancer Res*. 2002;86:41–65.
- [31] Weichert W. HDAC expression and clinical prognosis in human malignancies. *Cancer Lett*. 2009;280(2):168–176.
- [32] Osada H, Tatematsu Y, Saito H, et al. Reduced expression of class II histone deacetylase genes is associated with poor prognosis in lung cancer patients. *Int J Cancer*. 2004;112(1):26–32.
- [33] Ouaiissi M, Sielezneff I, Silvestre R, et al. High histone deacetylase 7 (HDAC7) expression is significantly associated with adenocarcinomas of the pancreas. *Ann Surg Oncol*. 2008;15(8):2318–2328.
- [34] Barneda-Zahonero B, Parra M. Histone deacetylases and cancer. *Mol Oncol*. 2012;6(6):579–589.
- [35] McMahon SB, Van Buskirk HA, Dugan KA, et al. The novel ATM-related protein TRRAP is an essential cofactor for the c-Myc and E2F oncoproteins. *Cell*. 1998;94(3):363–374.
- [36] Frank SR, Parisi T, Taubert S, et al. MYC recruits the TIP60 histone acetyltransferase complex to chromatin. *EMBO Rep*. 2003;4(6):575–580.
- [37] Su R, Gong JN, Chen MT, et al. c-Myc suppresses miR-451 YWTAZ/AKT axis via recruiting HDAC3 in acute myeloid leukemia. *Oncotarget*. 2016;7(47):77430–77443.
- [38] Rountree MR, Bachman KE, Herman JG, et al. DNA methylation, chromatin inheritance, and cancer. *Oncogene*. 2001;20(24):3156–3165.
- [39] Kelland L. The resurgence of platinum-based cancer chemotherapy. *Nat Rev Cancer*. 2007;7(8):573–584.
- [40] Efferth T. Resistance to targeted ABC transporters in cancer. Springer International Publishing Switzerland; 2015.
- [41] Yu Q, Liu Y, Zheng X, et al. Histone H3 lysine 4 trimethylation, lysine 27 trimethylation, and lysine 27 acetylation contribute to the transcriptional repression of solute carrier family 47 member 2 in renal cell carcinoma. *Drug Metab Dispos*. 2017;45(1):109–117.
- [42] Chen MY, Liao WS, Lu Z, et al. Decitabine and suberoylanilide hydroxamic acid (SAHA) inhibit growth of ovarian cancer cell lines and xenografts while inducing expression of imprinted tumor suppressor genes, apoptosis, G2/M arrest, and autophagy. *Cancer*. 2011;117(19):4424–4438.
- [43] Dong Y, Desmond JC, Ong JM, et al. Suberoylanilide hydroxamic acid (SAHA) crosses the blood-brain barrier and inhibits growth of human multiforme glioblastomas in the brains of immunodeficient mice. *Cancer Res*. 2005;65:S771.
- [44] Paddison PJ, Cleary M, Silva JM, et al. Cloning of short hairpin RNAs for gene knockdown in mammalian cells. *Nat Methods*. 2004;1(2):163–167.
- [45] Richon VM, Webb Y, Merger R, et al. Second generation hybrid polar compounds are potent inducers of transformed cell differentiation. *Proc Natl Acad Sci USA*. 1996;93(12):5705–5708.
- [46] Foltman M, Sanchez-Diaz A. Studying protein-protein interactions in budding yeast using co-immunoprecipitation. *Methods Mol Biol*. 2016;1369:239–256.
- [47] Plumb JA. Cell sensitivity assays: the MTT assay. *Methods Mol Med*. 1999;28:25–30.